Colloids and Surfaces A: Physicochem. Eng. Aspects 333 (2009) 126–132

Contents lists available at ScienceDirect

Colloids and Surfaces A: Physicochemical and Engineering Aspects

journal homepage: www.elsevier.com/locate/colsurfa

Preparation and characterization of silver thiocyanate – tetrabromo-tetrachlorofluorescein inclusion material and its adsorption to synthetic dye

Hong-Yan Wang, Li-Min Ma, Tian Li, Ya-Lei Zhang, Hong-Wen Gao*

State Key Laboratory of Pollution Control and Resource Reuse, College of Environmental Science and Engineering, Tongji University, Shanghai 200092, China

ARTICLE INFO

Article history:
Received 25 November 2007
Received in revised form
14 September 2008
Accepted 15 September 2008
Available online 27 September 2008

Keywords:
Tetrachloro-tetrabromofluorescein
Silver thiocyanate
Ethyl violet
Inclusion material
Adsorptive precipitation
Dye adsorption

ABSTRACT

From the adsorptive precipitation of SCN^-, tetrachloro-tetrabromofluorescein (TBTCF) and Ag^+, we found *in-situ* embedment of TBTCF into growing silver thiocyanate particles to form ternary electronegative inclusion material. The composition, size and phase of the material were determined by spectrophotometry and ICP and characterized by XRD, SEM, etc. The results showed that *in-situ* inclusion particles $\{[Ag(SCN)]_m(TBTCF)\}_n^{2n-}$ ($m = 33 \pm 11$) were formed. The inclusion particles adsorbed cationic dyes selectively and rapidly. A representative cationic dye, ethyl violet (EV), was used to investigate the performance of the ternary inclusion particles and the mechanism involved. The equilibrium adsorption capacity of the Ag(SCN)/TBTCF inclusion particles is 202 mg/g EV, over 14 times higher than absorption to the silver thiocyanate–only particles and slightly more than activated carbon. Moreover, the adsorption approached the equilibrium in 10 min, which is much less than that with activated carbon in about 2 h. In this work, a simple preparation method of the inclusion material as dye adsorbent was established and it will play an important role in the removal or recovery of cationic organic substances from aqueous.

1. Introduction

Environmental pollution today has far-reaching negative consequences on human lives. Degradation of organic pollutants that have deleterious effects on human well-being has become a focus of current scientific research effort. Pollutants emitted from various sources pose severe ecological problems because their bio-degradation is often very slow and conventional treatments are mostly ineffective and not environmentally compatible [1]. Dye pollutants are an important source of environmental contamination. Over 100,000 dyes have been made and more than 7×10^5 tones are produced annually [2]. More than 10,000 dyes are commercially available and 5–10% of these are discharged into wastewaters by textile industries [3]. Dye wastewaters offer considerable resistance to biodegradation because the dyestuffs are synthetic aromatic compounds containing a variety of functional groups and are resistant to light, heat and oxidation agents. Some dyes are reported to cause allergy, dermatitis, skin irritation, cancer and mutations in humans [4,5]. Thus, it is important to remove dyes from effluents before they mix with unpolluted natural water bodies.

Physico-chemical processes are generally used to treat dye-laden wastewater. These processes include flocculation, electroflotation, precipitation, electro-kinetic coagulation, ion exchange, membrane filtration, electrochemical destruction and irradiation [6]. Increasing numbers of novel environmental materials are being found for removing organic dyes, such as nano-sized TiO_2 photocatalysts [7,8]. However, all these processes are costly and cannot be used by small industries to treat a wide range of dye wastewaters [9]. Adsorption is one of the most efficient methods of removing pollutants from wastewater [10,11]. Adsorbents may be of natural, mineral, organic or biological origin [12]. Many different types have been found to be effective in removing certain colors from aqueous effluents. Activated carbon has been used most commonly [13,14] because of its high adsorption capacity, though its cost is also high. Other natural biosorption materials have also been investigated [15–21]. Recently, several new and efficient types of adsorbents have been synthesized, for example polymer and resin [22,23], magnetic [24] and modified natural materials [25]. Ever since the adsorption technique was first used to remove toxic chemicals from wastewater there have been efforts to find new, economic and competent adsorbents, particularly waste materials. Thus, many waste materials such as shells, husks, plant leaves, etc. have been tried as adsorbents.

Some well-known adsorptive precipitation reactions with color indicators were developed in the middle of the last century and

* Corresponding author. Tel.: +86 21 65988598; fax: +86 21 65988598.
E-mail address: hwgao@mail.tongji.edu.cn (H.-W. Gao).

0927-7757/$ – see front matter © 2008 Elsevier B.V. All rights reserved.
doi:10.1016/j.colsurfa.2008.09.039

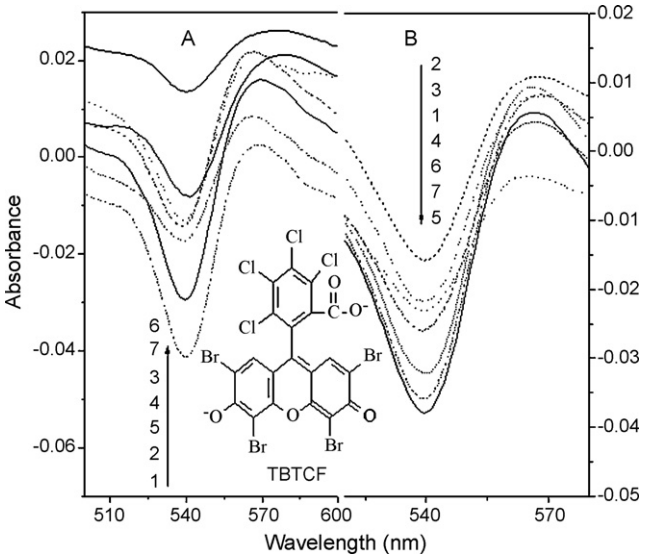

Fig. 1. (A) Absorption spectra of reactions of Ag^+ (20.0 μg/ml), SCN^- (1.0 μg/ml) and TBTCF (0.0100 μmol/ml) in various pH media from 1 to 5: pH 3.36, 3.81, 4.39, 4.96, 5.51 and 1.0 in the addition subsequence SCN^--$TBTCF^{2-}$-Ag^+. 6: the same as A2 but in the addition subsequence SCN^--Ag^+-$TBTCF^{2-}$. 7: The same as A2 but in the addition subsequence Ag^+-$TBTCF^{2-}$-SCN^-. (B) The absorption spectra of the solution containing SCN^- (1.0 μg/ml), TBTCF (0.0100 μmol/ml) at pH 3.81 and Ag^+. From 1 to 7: 1.0, 3.0, 5.0, 10.0, 20.0, 30.0 and 50.0 μg/ml.

found early uses in Fajans titration of halogenides or thiocyanates [26,27]. However, we recently found that the mode of adsorption is not the only a surface binding type; the organic color adsorbate can enter the inner part of the precipitate by electrostatic attraction to form the ternary inclusion particles. This is quite important for preparing novel types of adsorbent. In the present work, tetrachloro-tetrabromofluorescein (TBTCF) (Fig. 1) was selected as the inclusion substance and the precipitation reaction between Ag^+ and SCN^- used for skeleton material. The structure, size and pattern of Ag(SCN)-TBTCF inclusion material were characterized by UV absorption, ICP, particle size analysis, XRD, and SEM. The adsorption of ethyl violet (EV) was used to investigate the removal of cationic dye with the inclusion material. The *in-situ* embedment adsorption material preparation (IEAMP) methodology was established to be helpful for us to develop new types of advanced adsorption materials.

2. Experimental

2.1. Materials and chemicals

Silver nitrate and potassium thiocyanate were of analytical grade purchased from Sinopharm Chemical Reagent Co., Ltd (Shanghai, China). Tetrachloro-tetrabromofluorescein was purchased from Shanghai Specimen Model Factroy (Shanghai, China). All other reagents were of analytical grade purchased from Sinopharm Chemical Reagent Co. Ltd. (Shanghai, China).

2.2. Equipments

The absorption spectra of TBTCF were recorded with a Model Lambda-25 Spectrometer (PerkinElmer Instruments, USA) with the UV-WinLab software (version 2.85.04). A Model Optima-2100DV ICP-OES (PerkinElmer Instruments, USA) was used to determine silver content in the inclusion particles. A Model Zetasizer Nano-Z Zeta-potential Analyzer (Malvern Instruments, UK) was used to measure the zeta-potentials of the particles. A Model TG16-WS centrifugal machine (Hunan Xiangyi Instruments, China) was used to separate the inclusion particles from solution. A Model LS230 Particle Size Analyzer (Beckman Coulter, USA) with a Model LFC-101 Laser Channel (Ankersmid Ltd., Holland) was used to measure the size distribution of the inclusion particles with the LS v3.29 operation software controlled by computer. A Model D/max2550VB3+/PC X-ray diffractometer (XRD) (Rigaku Intern. Co. Japan) was used for identification of the crystal structure and size. A Model Quanta 200 FEG SEM (FEI Co., USA) was used to size and pattern of the inclusion materials. A Model JY92-II Ultrasonic Cell Disruptor (Ningbo Xinzhi Instruments, China) was used to crush the AgSCN-only and inclusion particles for the similar particle size.

2.3. Addition subsequence of various solutions

All studies were carried out in 10.0 ml calibrated flasks to which 1.0 ml acetic acid-acetate buffer, pH 3.81 and other solutions were added according to the following three subsequences: SCN^- (10 μg)-$TBTCF^{2-}$ (0.100 μmol)-Ag^+ (200 μg), SCN^- (10 μg)-Ag^+ (200 μg)-$TBTCF^{2-}$ (0.100 μmol) and Ag^+ (200 μg)-$TBTCF^{2-}$ (0.100 μmol)-SCN^- (10 μg). Thus, the three Ag(SCN)-suspending liquids were prepared, respectively, and their absorption spectra were measured by spectrophotometry against the corresponding reagent without SCN^-. In addition, the liquids were centrifuged at 11,000 rpm and the precipitates washed with 20% DMF to remove TBTCF adsorbed on the particle surface. The final pellets were dissolved in ammonia solution and measured to estimate the occlusion of TBTCF in Ag(SCN) particles. The effects of pH and electrolytes on light absorption by the precipitates were investigated in order to find an optimal synthesis condition.

2.4. Determination of composition of the particles

Acetic acid-acetate buffer (1.0 ml, pH 3.81) was mixed in a series of flasks with 100 μg SCN^- and 0, 0.0050, 0.010, 0.020, 0.030, 0.050, 0.075, 0.10, 0.125, 0.150, 0.175 and 0.200 μmol $TBTCF^{2-}$ and diluted to approximately 5 ml with deionized water. Ag^+ (2 mg) was added and the mixture was diluted to 10 ml. After 10 min, the precipitates were centrifuged at 11,000 rpm. The absorbances of the supernatants were measured at 539 nm and thus the unbound TBTCF was determined. The precipitates were washed repeatedly with 50% DMF and centrifuged. The final pellets were dissolved in 0.4 ml ammonia solution and diluted to 10 ml. The Ag^+ and SCN^- concentrations in the clear solutions were measured by ICP-OES [28] and spectrophotometry. Simultaneously, the absorption of each solution was measured at 539 nm and the $TBTCF^{2-}$ concentration was calculated. Thus, the Ag/SCN and TBTCF/SCN molar ratios were calculated to characterize the adsorptive precipitates.

2.5. Preparation and characterization of particles

For convenient separation and easy use, micron-size ternary and Ag(SCN)-only particles were prepared. 5 mg of SCN^-, 7.5 μmol of TBTCF and 5.0 ml of pH 3.81 buffer were mixed and diluted to about 20 ml. 100 mg of Ag^+ was added. After reaction for 30 min, 25 ml of 50% DMF was added to dissolve the TBTCF only adsorbing on the particle surface. The supernatant was removed. Into the pellet, 25 ml of 50% DMF was added to again remove the surface adsorption of TBTCF and the liquid was diluted to 50 ml. According to the different addition sequences, the three liquids, respectively, containing Ag(SCN)-only, Ag(SCN)/TBTCF adsorption and Ag(SCN)/TBTCF inclusion particles were prepared. They were measured with a particle size analyzer for determining the particle size distribution and evaluating the aggregation of the crystal cells. Besides, the suspending particles in the liquids were separated by

centrifugation and dried and then the XRD and SEM of the Ag(SCN)-only and Ag(SCN)/TBTCF inclusion powders were measured.

2.6. Adsorption selectivity of particles

According the above preparation, after sedimentation of the three liquids for 30 min, the terminal pellets were re-suspended and dispersed in deionized water (50 ml) by ultrasonication for $x \times 10$ s (x is from 1 to 10) at 200 W interspersed until the target particles with the similar mean size were prepared in the three liquids. In addition, the SCN^- content in each of the liquids was determined by spectrophotometry. An acetic acid-acetate buffer (1.0 ml, pH 6) and one of liquids (1.0 ml) were mixed into 10 ml of dye solutions, two of which contained anionic dyes (0.010 μmol/ml acid violet 52 and 0.020 μmol/ml reactive brilliant red) and the others cationic dyes (0.030 μmol/ml EV and 0.050 μmol/ml new methylene blue). After centrifugation, the color change in each supernatant was compared with that of the corresponding dye solution.

The acetic acid-acetate buffer (1.0 ml, pH 6) and one of the particles liquids (1.0 ml) prepared above were added into a series of 10 ml solutions containing 0.100, 0.200, 0.300, 0.500, 0.700, 1.000, 1.500 and 2.000 ml of 0.100 mM EV. After mixed for 10 min, the mixtures were centrifuged at 11,000 rpm for 20 min and the excess EV in the supernatants was determined at 596 nm. The amounts of EV absorbed were calculated from the difference between the initial concentration and the excess free concentration of EV. Thus, appropriate adsorption models were established.

3. Results and discussion

3.1. Effect of the addition subsequences

Curves 1–5 in Fig. 1A show the absorption spectra of the solutions in various pH media according to the addition subsequence: SCN^--TBTCF-Ag^+. By comparing curve 2 with the others, the peak-valley absorbance interval is the most at pH 3.81. In this work, pH 3.81 buffer was used. From curve 6, the addition subsequence: SCN^--Ag^+-TBTCF was tried but the peak-valley absorbance interval was much less than the above subsequence. It is attributed to the fact that Ag(SCN) particles had been formed before the addition of TBTCF. TBTCF was adsorbed only onto the outer surfaces of the Ag(SCN) particles by colloidal electric double layers. From curve 7, the third addition subsequence: Ag^+-TBTCF-SCN^- achieved a less peak-valley absorbance interval than the first addition subsequence. The Ag(SCN) particles formed rapidly because the Ag^+ concentration (10 mg/l) remained high. Thus, there was not enough time for TBTCF to be adsorbed on the growing Ag(SCN) particles. However, in the addition subsequence: SCN^--TBTCF-Ag^+, only 1.00 mg/l SCN^- remained. When Ag^+ was added drop by drop, the Ag^+ concentration rose gradually from 0 to 10.0 mg/l. The formation of Ag(SCN) particles became slow so that TBTCF was adsorbed efficiently by the growing particles; moreover, it was embedded into them. From the chemical structure of TBTCF (Fig. 1), two negatively charged groups are favorable for the ion-pair attraction with Ag^+ and eight halogen substituents have a strong affinity to Ag^+. The free electrons of TBTCF embedded in the ternary particles would migrate towards the outer particle surface because of electrostatic induction [29]. This notable electron transfer of TBTCF resulted in both the obvious spectral red shift from 539 to 569 nm and the marked absorbance change in the first solution. From curves 1–7 in Fig. 1B, the peak-valley absorbance interval approached a maximum when the concentration of Ag^+ is over 20 times than that of SCN^-. Thus, SCN^- could be precipitated completely.

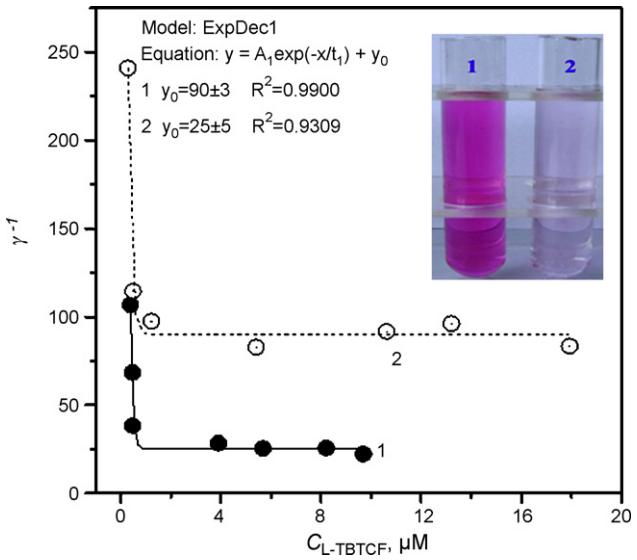

Fig. 2. Plots γ^{-1} vs. C_L of the solutions at pH 3.81containing 10.0 μg/ml SCN^-, 200 μg/ml Ag^+ and TBTCF from 0 to 0.020 μmol/ml. 1: the Ag(SCN)/TBTCF inclusion and 2: the Ag(SCN)/TBTCF adsorption system. Image 1: the Ag(SCN)/TBTCF inclusion and image 2: Ag(SCN)/TBTCT adsorption particles were dissolved in ammonia aqueous.

3.2. Inclusion of TBTCF into Ag(SCN) particles

The ternary reaction of TBTCF, Ag^+ and SCN^- may be expressed as:

$$N\text{TBTCF}^{2-} + \text{Ag}^+ + \text{SCN}^- \xrightarrow{K} \text{Ag(SCN)(TBTCF)}_N \downarrow$$
$$\text{Initiation}\quad C_{L0}(A^0_{539\,nm}) \quad C_{M0} \quad 0$$
$$\text{Equilibrium}\quad C_L(A_{539\,nm}) \quad C_M \to 0 \quad C_{M0}$$

where C_{L0} and C_{M0} are the initial molar concentrations of TBTCF and SCN^-, C_L and C_M are their molar concentrations at equilibrium, N is the saturating number of TBTCF molecules and K is the adsorption constant. C_L can be determined by measuring the absorbance of the centrifugal supernatant of the liquid at 539 nm. Thus, the molar ratio (γ) of TBTCF binding to the Ag(SCN) particles can be calculated by the relations:

$$\gamma = \eta \times \frac{C_{L0}}{C_{M0}} \tag{1}$$

where

$$\eta = \frac{C_{L0} - C_L}{C_{L0}} \tag{2}$$

The term η is the effective fraction of TBTCF binding to the Ag(SCN) particles. With increasing TBTCF concentration, γ will approach N. From plots γ^{-1} vs. C_L shown in Fig. 2, the surface adsorption of TBTCF on Ag(SCN) particles and its embedment plus surface adsorption in the Ag(SCN)/TBTCF inclusion particles remain the maximal constants when the molar ratio of TBTCF to SCN^- is more than 0.05. Thus, N of TBTCF is 0.040 ± 0.008 in the Ag(SCN)/TBTCF inclusion particles and 0.010 ± 0.002 in the Ag(SCN)/TBTCF adsorption particles. Thus, the saturation embedment of TBTCF in the inclusion particles is 0.03 ± 0.01/mol SCN^-. It means that mean 33 SCN^- molecules would bind with only one TBTCF molecule, i.e. the ternary inclusion particles $\{[\text{Ag(SCN)}]_m(\text{TBTCF})\}_n^{2n-}$ ($m = 33 \pm 11$) could be formed. Plots γ vs. C_L were fitted by the classical Temkin isotherm equation [30]:

$$\gamma = -\frac{NRT}{\Delta Q} \ln(KC_L) \tag{3}$$

$\Delta Q = Q^s - Q^0$, where Q^s and Q^0 are, respectively, the adsorption free enthalpies at saturation ($\gamma = N$) and the initial state ($\gamma = 0$), R is the gas constant (8.314 J mol^{-1} K^{-1}) and T the temperature (298.15 K). Both K and ΔQ were calculated as 1.17×10^7 M^{-1} and -10.5 kJ/mol for the Ag(SCN)/TBTCF inclusion particles and 1.71×10^7 M^{-1} and -9.3 kJ/mol for the Ag(SCN)/TBTCF adsorption particles, respectively. The adsorption of TBTCF is exothermic and the binding between TBTCF and Ag(SCN) particles is non-covalent from the little ΔQ values [31,32], involving e.g. affinity between Ag^+ and eight halogen groups of TBTCF, ion-pair attraction between Ag^+ and $-COO^-$ and $-O^-$ groups. Thus, TBTCF adsorbing during the growth of Ag(SCN) particles was not able to release immediately into aqueous so that it was embedded to form the inorganic–organic hybrid adsorption material.

To demonstrate the *in-situ* embedment of TBTCF, DMF [33] was used to remove all the TBTCF molecules adsorbed onto the outer surfaces of the Ag(SCN) particles and ammonia aqueous was then used to dissolve them, releasing any embedded TBTCF. Their images were given in Fig. 2. From the image of solution 2, the TBTCF adsorbing onto the surface of the Ag(SCN) particles may be removed by DMF. However from the image of solution 1, the ammonia solution of the ternary particles after wash with DMF indicated a concentrated TBTCF color. Therefore, the embedment of TBTCF into the Ag(SCN) particles was confirmed.

3.3. Composition, size and pattern of the particles

For convenient for separation and easy to use, micron-size ternary and Ag(SCN)-only particles were prepared according to the same procedures as the first solution above, involving centrifugation of the particles and surface-washing with water. These particles were dissolved in ammonia aqueous for determination of Ag^+, SCN^- and TBTCF. The concentration of SCN^- was determined by colorimetry with Fe^{3+} [34] to be 0.304 mg/ml of the Ag(SCN)-only particles liquid, 0.226 mg/ml of the Ag(SCN)/TBTCF adsorption particles liquid and 0.142 mg/ml of the Ag(SCN)/TBTCF inclusion particles liquid. These were used to calculate the equilibrium adsorption capacity of the particle materials. TBTCF was determined by spectrophotometry and Ag^+ by ICP. The molar ratios of Ag^+ to SCN^- and TBTCF in these particles are calculated to be 0.91:1:0 for the Ag(SCN)-only particles, 0.97:1:0.042 for the Ag(SCN)/TBTCF adsorption particles and 0.95:1:0.081 for the Ag(SCN)/TBTCF inclusion particles. The addition of TBTCF has not affected the ratio of Ag^+ to SCN^- at constant 1:1. Thus, the embedment of TBTCF into the Ag(SCN) particles is 0.039/mol of Ag(SCN), i.e. 50% TBTCF was embedded into the Ag(SCN) particles. As a result, only one TBTCF molecule could be included into 26 Ag(SCN) molecules, which is in the above N scope. The Ag(SCN)/TBTCF inclusion particle, $\{[Ag(SCN)]_{26}(TBTCF)\}_n^{2n-}$ was formed, where the binding of TBTCF is non-covalent. Besides, the Zeta-potentials of the Ag(SCN), Ag(SCN)/TBTCF adsorption and the Ag(SCN)/TBTCF inclusion particles were measured to be -29.11, -50.04 and -40.60 mV. Thus, the Ag(SCN)/TBTCF inclusion particles carried the most negative charges and the Ag(SCN)-only particles aggregated most easily.

The size distribution of the suspending articles was measured as shown in Fig. 3. From Fig. 3A, over 70% of the Ag(SCN)-only particles are over 3 μm in diameter and approximately 0 more than 5 μm of diameter. However, from Fig. 3B and C over 50% of the adsorption and inclusion particles are less than 2 μm in diameter but the diameter range became very wide from 0.6 to 10 μm, in which 20% of particles are more than 5 μm. Increase of particle size is favorable for separation of particles. These indicated that the addition of TBTCF altered the surface property of particles to result in change of the crystal cell aggregation ability. From the XRD data in Fig. 4,

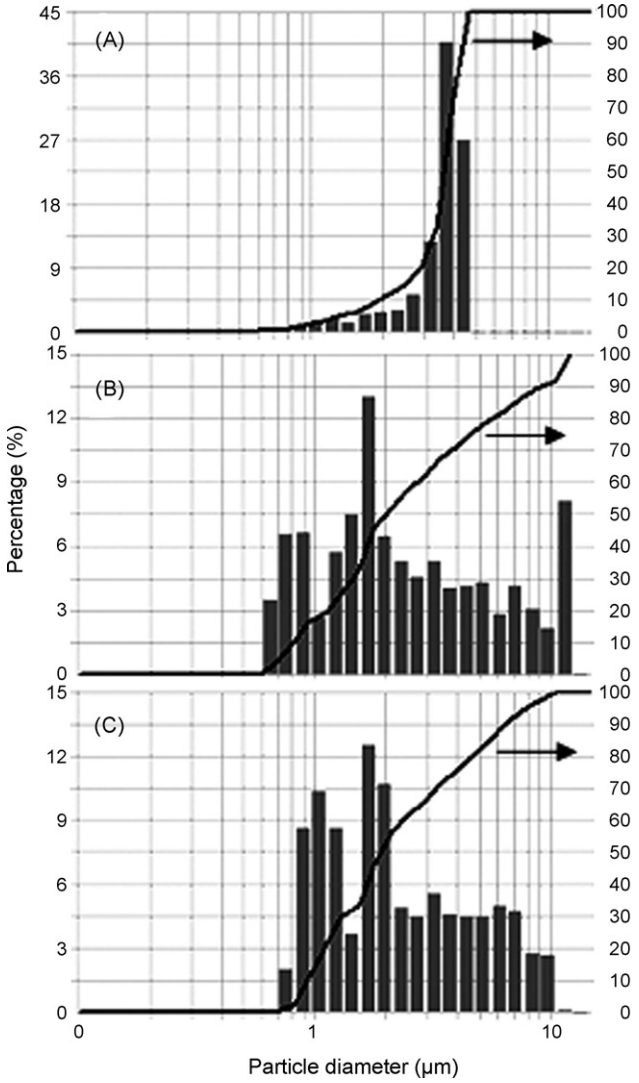

Fig. 3. Size measurement of the Ag(SCN)-only (A), Ag(SCN)/TBTCF adsorption (B) and Ag(SCN)/TBTCF inclusion (C) particles.

the mixing of TBTCF has not altered the crystallization process and crystal-cell phase of Ag(SCN) because all the diffraction angles have no change. Moreover, the doping of TBTCF reduced obviously the particle size by comparison of the diffraction peak half-width values. However, from the higher peaks around 30° of 2θ angle the elemental silver and its oxide may be formed after the particle powder was separated and exposed in air. From SEM image A in Fig. 4, the Ag(SCN) particles are so non-uniform and they cement easily into big sheets between 1 and 2 μm. On the contrary, from SEM image B, the Ag(SCN)-TBTCF particles are near-spherical and uniform being approximately 80 nm in size. As a result, the specific surface area of the ternary inclusion material is more than that of the Ag(SCN)-only particles.

3.4. Adsorption selectivity of the particles

Because of the obvious particle diameter difference in three reaction liquids (Fig. 3), the ultrasonication dispersion was carried out to form the stable and size-similar suspending particles, being convenient for the determination of absorption performance of organic dyestuffs under the equal specific surface condition. Two anionic dyes: acid violet 52 and reactive brilliant red, and

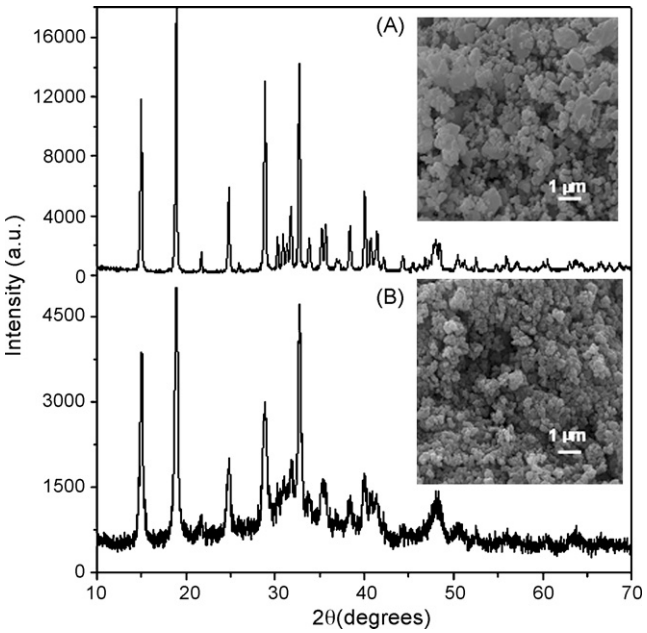

Fig. 4. Powder X-ray diffractogram and SEM images for Ag(SCN)-only (A) and Ag(SCN)/EY inclusion particles (B).

two cationic dyes: EV and new methylene blue, were added to the above suspensions of the Ag(SCN)-only particles, Ag(SCN)/TBTCF adsorption particles and the Ag(SCN)/TBTCF inclusion particles. Images of the supernatants after centrifugation of the liquids are shown in Fig. 5A–D. By comparing the color of solutions B1–B4 with that of solutions A1–A4, the Ag(SCN)-only particles has hardly removal effects of four dyes at pH 6. From solutions C1–C4, the Ag(SCN)/TBTCF adsorption particles can adsorb both EV and methylene blue but the TBTCF was released obviously into the solution. From solutions D1–D4, the Ag(SCN)/TBTCF inclusion particles have the most obvious adsorption of both EV and methylene blue at pH 6. From solutions 3 and 4 in A–D, both the anionic dyes: acid violet 52 and reactive brilliant red have hardly been removed. Thus, the adsorption of dye is mainly due to the electric field effect, i.e. the charge attraction controlled the adsorption capacity of dye. In a cationic solution, the free electrons of TBTCF embedded in the particles would move towards the outer particle surface by the electrostatic induction to form numerous micro-conductors [29,35], as illustrated in Fig. 5E. Electrostatic attraction to the particle surface results in the adsorption and enrichment of cationic dye (R^+). In contrast, anionic dye will not be attracted. Therefore, the Ag(SCN)/TBTCF inclusion particles are a kind of selective adsorbents that could be very useful for the removal and recovery of cationic dyes.

3.5. Adsorption of EV

The adsorption of EV was investigated in more detail onto the above three particles and the classical activated carbon at pH 6 and their plots γ^{-1} vs. $C_{L\text{-}EV}$ is shown in Fig. 6. The adsorption of EV on

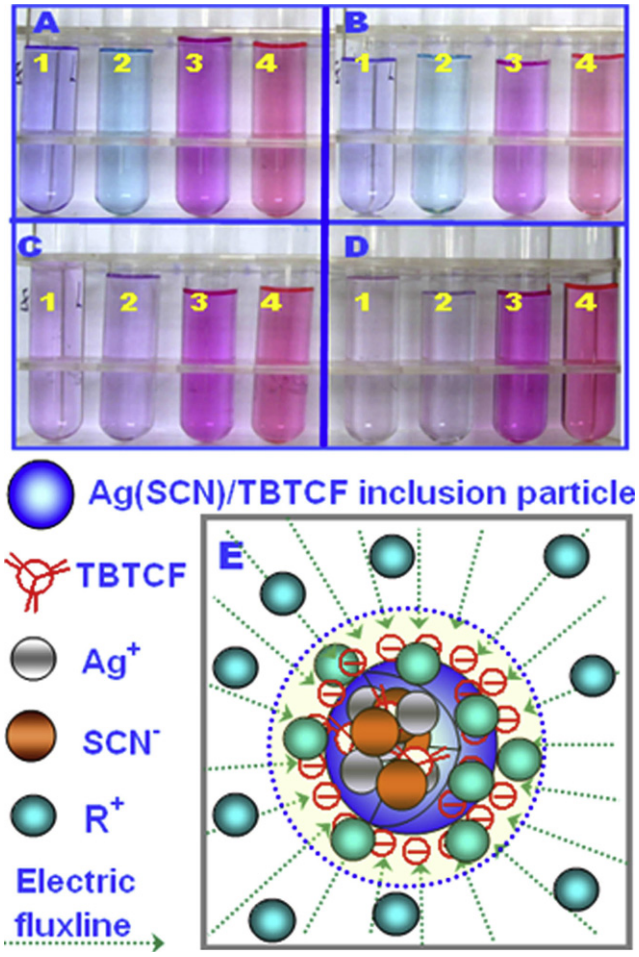

Fig. 5. Images of the supernatants centrifuged from the liquids initially containing (A) only dye, (B) dye and Ag(SCN)-only particles, (C) dye and Ag(SCN)/TBTCF adsorption particles and (D) dye and Ag(SCN)/TBTCF inclusion particles. 1.0 ml of each of the particle liquids was added into 10 ml the reaction tube. Dyes: 1–3 μM EV, 2–5 μM methylene blue, 3–10 μM acidic violet 52 and 4–20 μM reactive brilliant red. (E) Cartoon illustrating the electrostatic adsorption of cationic dye (R^+) onto the surface of the Ag(SCN)/TBTCF inclusion particles.

the Ag(SCN)-only particles approached the saturation from curve 1 when EV is more than 5 μM, that on the Ag(SCN)/TBTCF inclusion particles from curve 2 when EV is over 1.5 μM, that on the Ag(SCN)/TBTCF adsorption particles from curve 3 when EV is over 2 μM and that on activated carbon from curve 4 when EV is over 10 μM. *N* and equilibrium adsorption capacities of EV were calculated as given in Table 1. The Ag(SCN)/TBTCF inclusion particles adsorbed EV over 14 times more efficiently than the Ag(SCN)-only particles and nine times than the Ag(SCN)/TBTCF adsorption particles. The difference level at 179 mg EV between the Ag(SCN)/TBTCF inclusion particles and the Ag(SCN)/TBTCF adsorption particles must therefore result from the additional action of TBTCF *in-situ* embedding into the Ag(SCN) particles. Thus, *in-situ* embedment of TBTCF enhanced the adsorption performance markedly. By

Table 1
Adsorption constants of various adsorption materials with EV as the absorbate.

Adsorption materials	*N*	K ($\times 10^6$)	ΔQ (kJ/mol)	Equilibrium adsorption capacity/time (μg mg^{-1} EV/min)
Ag(SCN)-only particles	0.0050 ± 0.0002	2.09	−6.73	14/10
Ag(SCN)/TBTCF adsorption particles	0.010 ± 0.002	1.78	−7. 40	23/10
Ag(SCN)/TBTCF inclusion particles	0.10 ± 0.02	13.4	−13.7	202/10
Activated carbon	0.005 ± 0.001	5.58	−12.0	190/120

comparison of the Ag(SCN)/TBTCF inclusion particles and activated carbon, the equilibrium adsorption capacity of the Ag(SCN)/TBTCF inclusion particles is slightly more than that of the activated carbon. Besides, from Table 1, the adsorption of EV onto activated carbon is very slow and it spent for over 2 h to approach the equilibrium. However, the Ag(SCN)/TBTCF inclusion particles were complete in 10 min. Without doubt, the Ag(SCN)/TBTCF inclusion material provided an efficient and rapid removal or recovery of EV.

All plots γ vs. C_L were fitted by the classical Temkin isotherm equation and both K and ΔQ of the adsorptions were calculated as in Table 1. The adsorptions of EV by all the particles are non-covalent, spontaneous and exothermic. Comparison of the K and ΔQ values shows that EV interacts more strongly with the Ag(SCN)-TBTCF embedment particles than with the others, demonstrating that the *in-situ* inclusion material has a greater binding energy for the adsorbate. This is attributable to the charge attraction for EV by the electronegative Ag(SCN)-TBTCF micro-conductor (Fig. 5E), in addition to the electric double layer adsorption effect shared with the Ag(SCN)-only particles. As a result, the binding of EV to the Ag(SCN)/TBTCF inclusion particles may be very firm. This was confirmed from the effect of ion strength below.

3.6. Effect of pH and ionic strength

Fig. 7 shows the effects of pH and ionic strength on the adsorption of EV onto the three particles. From curve A1, γ of EV remains almost constant at about 0.013 and this indicated that the acidity did not affect the interaction of EV with the Ag(SCN)-only particles. From curves A2 and A3, γ of EV increased with increase in pH and then remained constant when pH is more than 6. γ of EV in neutral and basic media approaches over 1.5 times that at pH 1, i.e. the adsorption capacities of the Ag(SCN)/TBTCF inclusion particles and the Ag(SCN)/TBTCF adsorption particles raise obviously when pH is more than 6. It is attributed to the fact that the functional groups, e.g. $-COO^-$ and $-O^-$ of TBTCF, were protonized into –COOH and –OH in an acidic media. Thus, TBTCF species occluded

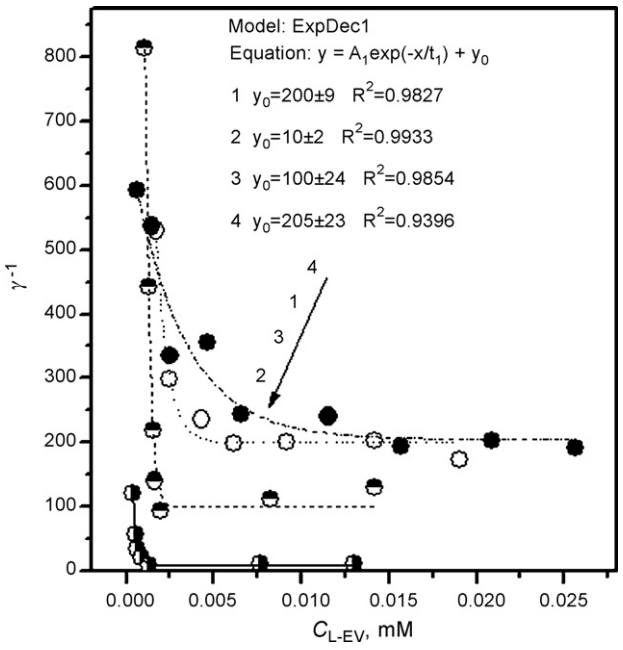

Fig. 6. Plots γ^{-1} vs. C_L for the adsorption of EV on the particles. 1: Ag(SCN)-only, 2: Ag(SCN)/TBTCF inclusion and 3: Ag(SCN)/TBTCF adsorption particles, and 4: activated carbon. 1.0 ml of each of the particle liquids was added into 10 ml the reaction tube.

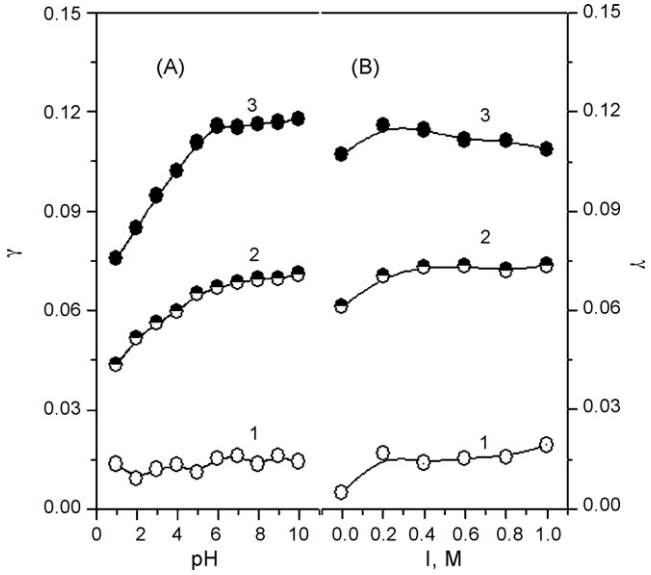

Fig. 7. Variation of γ of EV with pH (A) and ionic strength (B). 1: Ag(SCN)-only, 2: Ag(SCN)/TBTCF adsorption and 3: Ag(SCN)/TBTCF inclusion particles. 1.0 ml of each of the particle liquids and 10 μM EV were added into 10 ml the reaction tube.

in the Ag(SCN) particles decreased the attraction to cationic EV. As a result, the Ag(SCN)/TBTCF inclusion particles are more suitable for treatment of the neutral and basic wastewaters. From curves B1, B2 and B3, all changes of γ of EV are less than 20% with increase in the ionic strength from 0 to 1 M. Thus, the Ag(SCN)/TBTCF inclusion particles can be subject to impact of a high salt aqueous. As a result, the ternary inclusion particles can keep a stable adsorption capacity in a wide use environment.

4. Conclusions

By characterizing the SCN^--TBTCF-Ag^+ adsorptive precipitate using various modern instruments combined with isothermal adsorption model, the ternary *in-situ* inclusion particle $\{[Ag(SCN)]_m(TBTCF)\}_n^{2n-}$ ($m = 33 \pm 11$), an electronegative micron-sized adsorbent, was found to be selective and efficient in adsorbing cationic dyes. The Ag(SCN)/TBTCF inclusion belongs to the inorganic–organic hybrid adsorption material and it is different from the conventional ion-exchange resins or surface adsorbents because it raised greatly the adsorption efficiency by the synergistic adsorption of ion exchange and surface binding. Moreover, the adsorption is hardly subject to the impact of electrolyte and the binding particles were easy to be separated and treated. Although this work involves the use of silver, the ternary inclusion particles can be regenerated in diluted acid and then recycled for multiple uses. It overcomes the limitations and shortages of the conventional adsorbents, such as low adsorption capacity, too long saturation adsorption time, and difficult regeneration and poor recycle. This work provided a simple and potentially useful method for preparing efficient electronegative adsorbents to remove or extract organic substances, e.g. dye, medicine, active components from aqueous media.

Acknowledgments

We sincerely thank the State Key Laboratory Foundation of China Science and Technology Ministry (grant no. PCRRK08003) and the National Key Technology R&D Program of China (grant no. 2006BAJ08B10 and 2008BAJ08B13) for financially supporting this work.

References

[1] D. Chatterjee, S. Dasgupta, Visible light induced photocatalytic degradation of organic pollutants, J. Photochem. Photobiol. C 6 (2005) 186–205.
[2] G. McMullan, C. Meehan, A. Conneely, N. Kirby, T. Robinson, P. Nigam, I.M. Banat, R. Marchant, W.F. Smyth, Microbial decolourisation and degradation of textile dyes, Appl. Microbiol. Biotechnol. 56 (2001) 81–87.
[3] R.M. Gong, M. Li, C. Yang, Y.Z. Sun, J. Chen, Removal of cationic dyes from aqueous solution by adsorption on peanut hull, J. Hazard. Mater. B 121 (2005) 247–250.
[4] C. Sudipta, C. Sandipan, P.C. Bishnu, R.D. Akhil, K.G. Arun, Adsorption of a model anionic dye, eosin Y, from aqueous solution by chitosan hydrobeads, J. Colloid Interface Sci. 288 (2005) 30–35.
[5] J.P. Maloney, A.C. Halbower, B.F. Fouty, K.A. Fagan, V. Balasubramaniam, A.W. Pike, P.V. Fennessey, M.N. Moss, Systemic absorption of food dye in patients with sepsis, New Engl. J. Med. 343 (2000) 1047–1049.
[6] B. Noroozi, G.A. Sorial, H. Bahrami, M. Arami, Equilibrium and kinetic adsorption study of a cationic dye by a natural adsorbent – silkworm pupa, J. Hazard. Mater. B 139 (2007) 167–174.
[7] S. Senthilkumaar, K. Porkodi, Heterogeneous photocatalytic decomposition of crystal violet in UV-illuminated sol–gel derived nanocrystalline TiO_2 suspensions, J. Colloid Interface Sci. 288 (2005) 184–189.
[8] G. Sivalingam, K. Nagaveni, M.S. Hegde, G. Madras, Photocatalytic degradation of various dyes by combustion synthesized nano anatase TiO_2, Appl. Catal. B 45 (2003) 23–38.
[9] D.M. Indra, C.S. Vimal, K.A. Nitin, M.M. Indra, Adsorptive removal of malachite green dye from aqueous solution by bagasse fly ash and activated carbon-kinetic study and equilibrium isotherm analyses, Colloids Surf. A 264 (2005) 17–28.
[10] A.M. Mastral, T. Garcia, M.S. Callen, J.M. Lopez, M.V. Navarro, R. Murillo, J. Galban, Three-ring pah removal from waste hot gas by sorbents: influence of the sorbent characteristics, Environ. Sci. Technol. 36 (2002) 1821–1826.
[11] J.Y. Chen, D.Q. Zhu, C. Sun, Effect of heavy metals on the sorption of hydrophobic organic compounds to wood charcoal, Environ. Sci. Technol. 41 (2007) 2536–2541.
[12] P. Janos, Sorption of basic dyes onto iron humate, Environ. Sci. Technol. 37 (2003) 5792–5798.
[13] K. Mohanty, J.T. Naidu, B.C. Meikap, M.N. Biswas, Removal of crystal violet from wastewater by activated carbons prepared from rice husk, Ind. Eng. Chem. Res. 45 (2006) 5165–5171.
[14] C. Valderrama, J.L. Cortina, A. Farran, X. Gamisans, C. Lao, Kinetics of sorption of polyaromatic hydrocarbons onto granular activated carbon and Macronet hyper-cross-linked polymers (MN200), J. Colloid Interface Sci. 310 (2007) 35–46.
[15] S. Chatterjee, S. Chatterjee, B.P. Chatterjee, A.K. Guha, Adsorptive removal of congo red, a carcinogenic textile dye by chitosan hydrobeads: binding mechanism, equilibrium and kinetics, Colloids Surf. A 299 (2007) 146–152.
[16] Y.C. Wong, Y.S. Szeto, W.H. Cheung, G. McKay, Equilibrium studies for acid dye adsorption onto chitosan, Langmuir 19 (2003) 7888–7894.
[17] W.T. Tsai, K.J. Hsien, J.M. Yang, Silica adsorbent prepared from spent diatomaceous earth and its application to removal of dye from aqueous solution, J. Colloid Interface Sci. 275 (2004) 428–433.
[18] X. Yuan, S.P. Zhuo, W. Xing, H.Y. Cui, X.D. Dai, X.M. Liu, Z.F. Yan, Aqueous dye adsorption on ordered mesoporous carbons, J. Colloid Interface Sci. 310 (2007) 83–89.
[19] S.B. Wang, L. Li, H.W. Wu, Z.H. Zhu, Unburned carbon as a low-cost adsorbent for treatment of methylene blue-containing wastewater, J. Colloid Interface Sci. 292 (2005) 336–343.
[20] A.R. Cestari, E.F.S. Vieira, G.S. Vieira, L.E. Almeida, Aggregation and adsorption of reactive dyes in the presence of an anionic surfactant on mesoporous aminopropyl silica, J. Colloid Interface Sci. 309 (2007) 402–411.
[21] S.W. Won, S.B. Choi, B.W. Chung, D. Park, J.M. Park, Y.S. Yun, Biosorptive decolorization of reactive orange 16 using the waste biomass of *Corynebacterium glutamicum*, Ind. Eng. Chem. Res. 43 (2004) 7865–7869.
[22] E. Giménez-Martín, A. Ontiveros-Ortega, M. Espinosa-Jiménez, R. Perea-Carpio, Electrokinetic effect and surface free energy behavior in the adsorption process of a reactive dye onto Leacril pretreated with polyethyleneimine ion, J. Colloid Interface Sci. 311 (2007) 394–399.
[23] B.C. Pan, Q.X. Zhang, F.W. Meng, X.T. Li, X. Zhang, J.Z. Zheng, W.M. Zhang, B.J. Pan, J.L. Chen, Sorption enhancement of aromatic sulfonates onto an aminated hyper-cross-linked polymer, Environ. Sci. Technol. 39 (2005) 3308–3313.
[24] R.C. Wu, J.H. Qu, Y.S. Chen, Magnetic powder MnO-Fe_2O_3 composite-a novel material for the removal of azo-dye from water, Water Res. 39 (2005) 630–638.
[25] Q.Y. Yue, Q. Li, B.Y. Gao, Y. Wang, Kinetics of adsorption of disperse dyes by polyepicholorohydrin-dimethylamine cationic polymer/bentonite, Sep. Purif. Technol. 54 (2007) 279–290.
[26] R.C. Mehrotra, K.N. Tandon, Adsorption indicators in precipitation titrations, Talanta 11 (1964) 1093–1111.
[27] M.L. Baumann, A.L. Hatmaker, Ultramicro- and micro-determination of chloride by argentimetric titration with the indicator dichiorofluorescein, Clin. Chem. 7 (1961) 256–263.
[28] C.Z. Hang, B. Hu, Z.C. Jiang, N. Zhang, Simultaneous on-line preconcentration and determination of trace metals in environmental samples using a modified nanometer-sized alumina packed micro-column by flow injection combined with ICP-OES, Talanta 71 (2007) 1239–1245.
[29] A.H. Chen, H.T. Bi, J.R. Grace, Effects of charge distribution around bubbles on charge induction and transfer to a ball probe in gas–solid fluidized beds, J. Electrostat. 58 (2003) 91–115.
[30] C. Jeyaprabha, S. Sathiyanarayanan, K.L.N. Phani, G. Venkatachari, Influence of poly(aminoquinone) on corrosion inhibition of iron in acid media, Appl. Surf. Sci. 252 (2005) 966–975.
[31] G.L. Patrick, An introduction to medicinal chemistry., Oxford Univ. Press, London, 1995.
[32] M. Yang, Molecular recognition of DNA targeting small molecule drugs, J. Beijing Med. Univ. 30 (1998) 97–99.
[33] S.Z. Kang, Z.Y. Cui, J. Mu, High sensitivity to Cu^{2+} ions of electrodes coated with ethylenediamine-modified multi-walled carbon nanotubes, Nanotechnology 17 (2006) 4825–4829.
[34] E.B. Sandell, Colorimetric determination of trace metals, 3rd ed., Interscience Press, New York, 1959.
[35] S.X. Zhao, G.S. Peter Castle, K. Adamiak, Comparison of conduction and induction charging in liquid spraying, J. Electrostat. 63 (2005) 871–876.